ACS APPLIED MATERIALS & INTERFACES

Research Article

www.acsami.org

Carbon Nanotube Epoxy Nanocomposites: The Effects of Interfacial Modifications on the Dynamic Mechanical Properties of the Nanocomposites

Mitra Yoonessi,*[,†] Marisabel Lebrón-Colón,[‡] Daniel Scheiman,[§] and Michael A. Meador[‡]

[†]Ohio Aerospace Institute, 22800 Cedar Point Road, Cleveland, Ohio 44142, United States

[‡]NASA Glenn Research Center, 21000 Brookpark Road, Cleveland, Ohio 44135, United States

[§]ASRC, 21000 Brookpark Road, Cleveland, Ohio 44135, United States

ABSTRACT: Surface functionalization of pretreated carbon nanotubes (CNT) using aromatic, aliphatic, and aliphatic ether diamines was performed. The pretreatment of the CNT consisted of either acid- or photo-oxidation. The acid treated CNT had a higher initial oxygen content compared to the photo-oxidized CNT and this resulted in a higher density of functionalization. X-ray photoelectron spectroscopy (XPS) and thermal gravimetric analysis (TGA) were used to verify the presence of the oxygenated and amine moieties on the CNT surfaces. Epoxy/0.1 wt % CNT nanocomposites were prepared using the functionalized CNT and the bulk properties of the nanocomposites were examined. Macroscale correlations between the interfacial modification and bulk dynamic mechanical and thermal properties were observed. The amine modified epoxy/CNT nanocomposites exhibited up to a 1.9-fold improvement in storage modulus (G') below the glass transition (T_g) and up to an almost 4-fold increase above the T_g. They also exhibited a 3−10 °C increase in the glass transition temperature. The aromatic diamine surface modified epoxy/CNT nanocomposites resulted in the largest increase in shear moduli below and above the T_g and the largest increase in the T_g. Surface examination of the nanocomposites with scanning electron microscopy (SEM) revealed indications of a greater adhesion of the epoxy resin matrix to the CNT, most likely due to the covalent bonding.

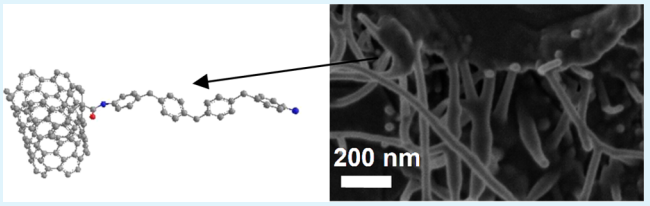

KEYWORDS: *carbon nanotube, epoxy, polymer nanocomposites, surface functionalization*

1. INTRODUCTION

Multifunctional polymer nanocomposites represent a class of functional materials with tailored properties that include enhanced thermal and mechanical stability, electrical conductivity and EMI shielding, diffusion and transport properties, and antivibration and damping.[1−7]Advanced technologies can be developed for lightweight applications such as aerospace structural components, jet engine parts, actuators, adaptive and smart materials, and robust durable materials using multifunctional polymer nanocomposites. The final properties of polymer nanocomposites are dictated by inherent properties of the constituents, interfacial area including physics, chemistry, and dynamics of interfaces, three dimensional orientations and spacing of the nanophase particles, and their particle particle interactions in multiple length scales. The nanoparticle inherent properties are its chemical composition, nanoparticle's size and dimensions, aspect ratio, and interfacial characteristics. The extent of dispersion or aggregation of the nanoparticles has a direct impact on the final properties of the polymer nanocomposites.

Epoxy resins and epoxy resin nanocomposites have been used in engineering structural components. Carbon nanotubes (CNT)/epoxy nanocomposites were reported in 1994[8] and since then there have been many reports for the thermal, mechanical, and electrical properties of CNT epoxy nanocomposites.[9−12]

Single wall carbon nanotubes (SWNT) are seamless rolled up graphene sheets with diameters of 1−10 nm, a Young's modulus of 0.32−1.47 TPa, strengths of 10−52 GPa, and a toughness of ∼770 J/g.[13−17] CNT are nonreactive due to their defect free, seamless arrangement of sidewall aromatic rings, which can lead to CNT aggregation. Poor dispersion of the CNT in the host resin results in poor properties of the polymer nanocomposite. Aggregation translates into lower available surface area, less interfacial interactions of CNT with the polymer molecules, stress concentrations, and lack of stress transfer.

Interfacial modifications have been critical to the dispersion of CNT in the epoxy resin matrix and have drastic effects on the physical and mechanical properties of the CNT epoxy nanocomposites.[18−21] Molecular design of interfacial chemistry is required to control the thermal and mechanical properties of high performance nanocomposites. The mechanisms governing interfacial phenomena are complex and not well understood. The interface is designed for targeted property enhancement in

Received: May 28, 2014
Accepted: September 12, 2014
Published: September 12, 2014

the specific polymer matrix. A recent study utilized Hansen solubility parameters to understand the interfacial modifications and dispersion of CNT in different polymer matices.[18] Small-molecule functionalized and electron-beam irradiated long CNT yarns epoxy resin composites have resulted in 25% and 88% increase in tensile moduli and strength for small molecule functionalized CNT yarn epoxy composite, and 57% and 48% improvements in tensile moduli and tensile strength for electron beam irradiated CNT yarn epoxy composites.[21]

Several strategies have been utilized for nanoparticles' functionalization. The most common methods of CNT functionalization are generation of functional sites using acid mixtures,[22] peroxides,[23] plasmas,[19] and photo-oxidation.[24] These methods generate oxygenated functional sites for the next step of chemical reactions, grafting of chemical moieties. A pristine carbon nanotube can also be modified using secondary interactions such as van der Waals interactions ($\pi-\pi$ stacking of compounds containing benzene rings with CNT),[25] or electrostatic interactions (surfactants).[26] These types of surface modification are generally performed while maintaining pristine sp^2 hybridization of the CNT for electrical and thermal properties. Some polymers have a specific helical configuration with a helix size the same diameter as the CNT. These polymers have been demonstrated to wrap around the CNT.[27] This type of modification does not damage the structure of CNT.

The grafting approach uses a chemical moiety covalently bonded to functional groups on the CNT surface generated by prior chemical or irradiation methods. This chemical moiety could be a small molecule or a longer chain designed molecule with a monofunctional reactive end group. Grafting can be utilized to attach an initiator to the nanoparticle surface where polymerization starts and results in CNT surface polymerization. The CNT surface initiator could be an atom transfer radical polymerization agent (ATRP) or reversible addition–fragmentation chain transfer (RAFT) agent where the polymerization of monomers starts.[28]

The strategy for nanoparticle interfacial modification is determined by the targeted properties of interest. Fluorination of carbon nanotubes resulted in their enhanced dispersion in epoxy and an enhanced modulus and tensile strength using only 1 wt % of the F-CNT.[29] Silanization of the carbon nanotube was performed using 3-aminopropyl trimethoxysilane (APTES),[30] both APTES and silica,[31] and more recently, by supercritical reaction of 3-(glycidyloxypropyl)trimethoxysilane (GPTMS).[32] This resulted in enhanced thermal mechanical properties. Carboxylic functionalized CNT infiltrated into epoxy carbon fiber composites prepared using vacuum-assisted resin transfer molding showed a 40% increase in shear strength with 0.5 wt % COOH–CNT.[33] These epoxy COOH–CNT nanocomposites demonstrated improved dispersion and higher electrical and thermal conductivity.[34]

Amidation has been widely used to functionalize CNT. Ethylene diamine terminated CNT were used for binding to DNA and biological moieties.[35] Amine functionalized CNT dispersed in epoxy resulted in epoxy nanocomposites with higher flexural modulus and thermal mechanical properties.[35−38]

Maleic anhydride functionalized plasma treated CNT were treated with a diamine curing agent to generate a cross-linker with amine end groups. The CNT–MA–NH_2 was dispersed in an epoxy and used in the epoxy resin composite.[37] The CNT–MA–NH_2 epoxy nanocomposite exhibited improved thermal, mechanical, and electrical performance.[37] Differential scanning calorimetry and calculated thermodynamic parameters indicated that the diamines on the sidewalls of the CNT participated in cross-linking whereas the tip/end diamines functional groups did not.[38]

In this study, a novel systematic grafting method based on amine functionalization was used to generate CNT epoxy resin nanocomposites with covalent bonding between the epoxy resin matrix and the CNTs. CNT interfaces were modified with aliphatic, aliphatic ether, and aromatic diamines to generate series of interfaces with systematic changes in rigidity, polarity, and mobility. The effects of the density of functionalization on the properties were investigated. These interfaces were semiquantitatively characterized by thermal gravimetric analysis (TGA), X-ray photoelectron spectroscopy (XPS), and Fourier transform infrared spectroscopy (FT-IR). Attempts were made to correlate the interfacial characteristics such as chain polarity, mobility, and rigidity with the thermal and mechanical properties of the CNT epoxy nanocomposites.

2. EXPERIMENTAL SECTION

2.1. Materials. Carbon nanotubes (XM2334A), 2.5–3.8 nm diameters, containing 4–5 wt % Fe and Co catalyst were obtained from Carbon Nanotechnology Incorporated (CNI). Diglycidyl ether bisphenol A epoxy resin, Epon 826 (Resolution Performance Products), polypropylene glycol diamine, and Jeffamine D230, molecular weight of 230 (Huntsman Chemicals) were used as received. Sulfuric acid (36 M), nitric acid (15.8 M), 1,12-diaminododecane, 4,7,10-trioxa-1,13-tridecanediamine, *N,N′* dimethylformamide (DMF), thionyl chloride, and toluene from Sigma were used as received. 4,4′-(4,4′-Methylenebis(4,1-phenylene)bis-(methylene))dianiline had been synthesized in our laboratory.

2.2. CNT Surface Modification. CNT were modified with a mixture of sulfuric and nitric acid (3:1, v/v) at 65 °C based on a published procedure to generate oxidized CNT (OCNT).[22] The photo-oxidized CNT were prepared by exposing the CNT to ultraviolet light. The irradiation was for 24 h and is a nondestructive method of generating oxygenated functional groups reported elsewhere (POCNT).[24] The carboxylic groups of these oxidized CNT were converted to acid chloride by refluxing in thionyl chloride solution for 24 h. CNT functionalized with acid chloride were washed with anhydrous toluene and dried under vacuum. Then, these CNT were dispersed in anhydrous DMF, followed by the addition of the chosen diamines. The mixtures were refluxed for 24 h, washed until excess diamines were removed, and then dried.

2.3. Nanocomposite Preparations. Functionalized CNT were dispersed in DMF by sonication for 1.5 h. This was followed by the addition of Epon 826 and further sonication for another 30 min. Solvent was removed, and then the samples were placed in the vacuum oven overnight at 90 °C to ensure complete solvent removal. The dispersions of CNT Epon were further sonicated. Then, Jeffamine D230 was added to the Epon/CNT dispersions and placed under vacuum for degassing for 45 min. The samples were cured at 75 °C for 2 h and 125 °C for 2 h, followed by a postcuring. This method resulted in epoxy CNT nanocomposites containing 0.1 wt % functionalized CNT.

2.4. Characterization and Instruments. A TA Instruments Q500 thermogravimetric analyzer was used under nitrogen from 25 to 800 °C with a scan rate of 10 °C/min. X-ray photoelectron spectroscopy (XPS) was performed using an EscaLab 200 instrument with a scanning microprobe and a Mg Kα radiation (1253.6 eV) focused source with a 180° hemispherical electron energy analyzer. Survey scans and high resolution spectra of C 1s, N 1s, and O 1s were obtained. The atomic percentage ratio values were calculated from the high resolution spectra. Shirley background subtraction, shift of data sets based on 284.6 eV, atomic percentage based on survey scans, and peak deconvolution of high resolution spectra were performed. The

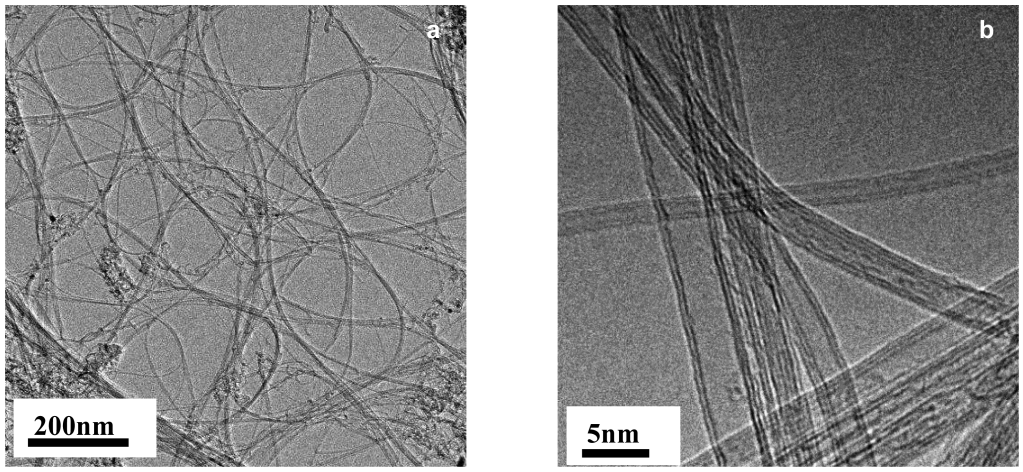

Figure 1. (a) Entangled CNT carbon nanotubes with long lengths. (b) Carbon nanotubes are predominantly double wall with some triple walls.

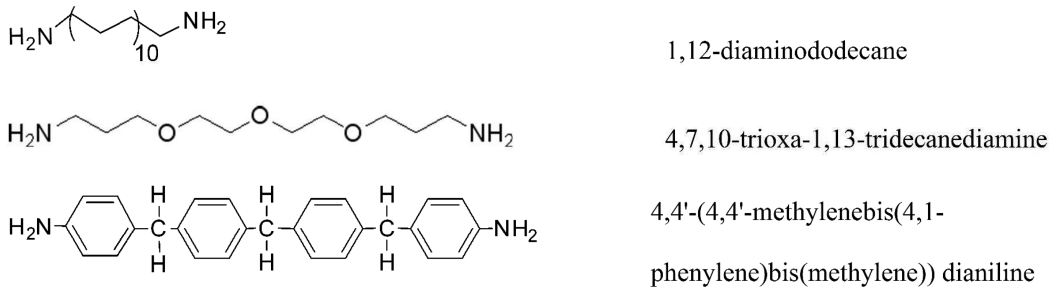

2a. Chemical structure of diamines

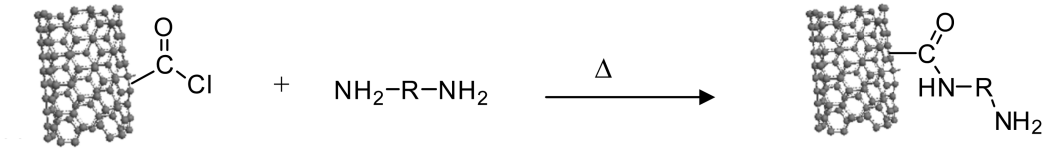

2b. Acyl chloride functionalized CNT reacted with diamine and generated amine functionalized CNT

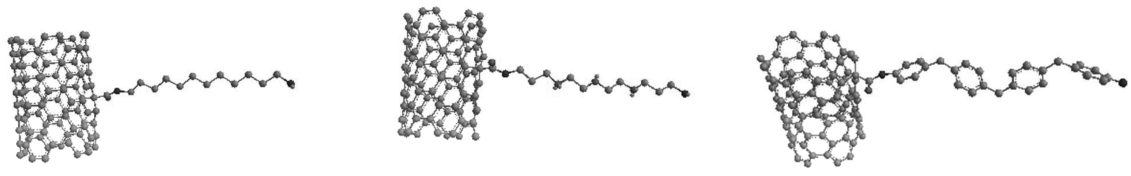

2c. Schematics of C12-CNT, aliphatic ether-CNT, and Ph4-CNT

Figure 2. Schematic of (a) three types of diamine, (b) reaction of acyl chloride OCNT (or POCNT) with diamines, and (c) three amine modified CNT.

dynamic mechanical data were obtained using ARES rheometer in shear mode from room temperature to 200 °C at 1 Hz frequency. High resolution transmission electron microscopy (HR-TEM) of the nanoparticles was performed using a Philips CM200 instrument. Scanning electron microscopy (SEM) was performed using a FEG-SEM Hitachi instrument on carbon coated fracture surfaces.

3. RESULTS AND DISCUSSION

3.1. CNT Characterization. *3.1.1. HR-TEM.* TEM micrographs of as-received CNT (Figure 1a,b) show the presence of extremely long double wall carbon nanotubes with a few single walls, triple, and some multiwall CNT. Carbon nanotubes have an extremely large surface area (SWNT, 1315 m^2/g; double wall NT, 700−800 m^2/g).[13] As-received CNT are mostly double walled with ∼700−800 m^2/g surface area. CNT were

dx.doi.org/10.1021/am5056849 | ACS Appl. Mater. Interfaces 2014, 6, 16621−16630

treated with two methods to generate oxygenated functional groups on the CNT nanotube surface for grafting. In the first method, a mixture of sulfuric and nitric acid (v/v, 3:1), combined with heat and sonication was used.[22] In second method, oxidation of CNT by means of photoirradiation was utilized.[24] Treatments of CNT with both methods generate oxygenated functional groups, i.e., carboxylic groups on CNT surface.

Oxidized carbon nanotubes have carboxylic groups on the CNT surfaces that were used for reaction with diamines. First, these carboxylic groups were converted to acid chloride to enhance the reactivity, and then reacted with diamines. The chemical structures of the diamines, the reaction scheme of diamine with acyl chloride functionalized CNT, and the surface modified OCNT and POCNT with diamines are presented in Figure 2a,b,c. The acyl chloride CNT reacted with three types of diamines, aliphatic diamine with 12 carbon atoms, 1,12-diaminododecane (C12-OCNT), aliphatic ether diamine, 4,7,10-trioxa-1,13-tridecanediamine (aliphatic ether-OCNT), and 4,4′-(4,4′-methylenebis(4,1-phenylene)bis(methylene))-dianiline (Ph4-OCNT).

3.1.2. TGA. Figure 3 shows the TGA of the as-received CNT compared with the functionalized CNT. TGA analysis of the as-

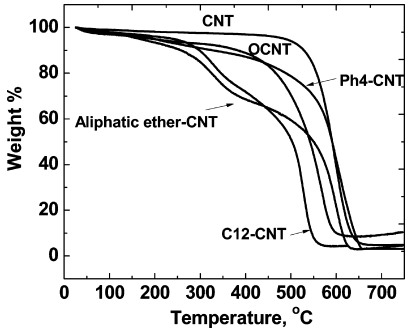

Figure 3. TGA of as received CNT, acid treated CNT, OCNT, Ph4-OCNT, C12-diamine-CNT, and aliphatic ether diamine-OCNT.

received CNT showed a thermal stability up to 598 °C (onset of decomposition). Acid treated CNT have a weight loss starting at ∼197 °C where the weight steadily decreases to 86.5% at 473 °C. The initial weight loss is due to the presence of the additional oxygenated functional groups on the CNT surface that gradually decompose and oxidize. The C12-OCNT and aliphatic ether-OCNT exhibited initial decomposition temperatures of 330 and 321 °C. This lower temperature decomposition indicates the presence of the aliphatic hydrocarbon chain on the CNT surfaces. The aliphatic ether-OCNT exhibited an even lower starting decomposition temperature, perhaps due to the lower energy carbon oxygen bonds. These CNT showed a plateau at temperatures >400 °C, until they reached temperatures above 500 °C, where the complete decomposition of CNT occurred. TGA has been widely used to determine the organic content of surface functionalized CNT.[32,38]

The aromatic diamine treated CNT, Ph4-OCNT, did not show any weight loss up to 596 °C. Aromatic treated diamine, Ph4-OCNT, showed low temperature decomposition similar to acid treated CNT, but improved thermal stability at temperatures above 500 °C. The improved thermal stability of the Ph4-OCNT at higher temperatures is attributed to the presence of aromatic groups on the CNT surfaces.

3.1.3. XPS. The surfaces of as received CNT, acid treated CNT, and the diamine modified CNT were examined by XPS (Figure 4). The acid treated CNT exhibited 8.4% of atomic

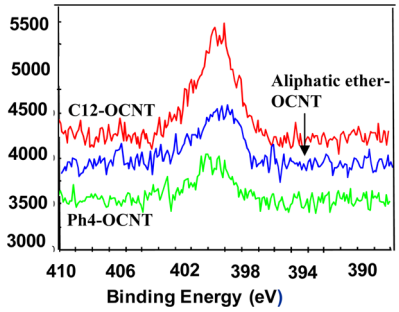

Figure 4. High resolution spectra of N 1s, C12-OCNT (red line), aliphatic ether-OCNT (blue line), and Ph4-OCNT (green line).

oxygen compared to >3% atomic oxygen of the as-received CNT, determined by high resolution spectra of O 1s. The POCNT exhibited 3.4% oxygen on the surface. The carbon-to-oxygen ratios of as-received CNT, photo-oxidized CNT, and acid treated CNT were 31.3/1, 28.4/1, and 10.9/1. Acid treated CNT showed the highest level of oxygen content and highest level of oxygenated functional groups on the surface.

Survey scans of diamine modified CNT showed the presence of C 1s, N 1s, and O 1s where nitrogen was absent in the as-received and acid modified CNT. The atomic percentages of the elements in diamine modified CNT were obtained from the high resolution scans are summarized in Table 1. The presence

Table 1. Elemental Analysis of Nitrogen Present on the Surface of Diamine Modified CNT

functionalized CNT	nitrogen, %
C12-OCNT	4.00
C12-POCNT	2.75
Ph4-OCNT	2.06
Ph4-POCNT	1.56
Aliphatic ether-OCNT	3.06
Aliphatic ether-POCNT	1.34

of nitrogen was only detectable for the diamine modified CNT. Table 1 shows the nitrogen content of the diamine treated CNT with starting OCNT and POCNT. This study allows us to compare the effects of the initial oxygenated functional group on the functionalization surface density. The CNT that were originally treated with acid exhibited a higher nitrogen percent compared to the functionalized CNT modified with starting photo-oxidized CNT. The nitrogen percentage for the diamine treated CNT prepared from acid treated CNT was in the range of 2−4%. The nitrogen percentage of the diamine functionalized CNT prepared from photo-oxidized CNT showed lower nitrogen content in the range of 1.34−2.75%. This is attributed to the high number of carboxylic groups on the surface of acid treated CNT and therefore, increased number of diamine covalently bonded on the CNT surfaces.

Deconvolution of C 1s high resolution spectra of OCNT and aliphatic ether-OCNT are presented in Figure 5a,b, respectively. Figure 5a shows peaks corresponding to the binding energies of 284.6, 285.4, and 289.9 eV corresponding to graphite carbon, β-carbon, and carbonyl/carboxylic acid.[39−41] Figure 5b shows the deconvoluted peaks for the aliphatic ether-

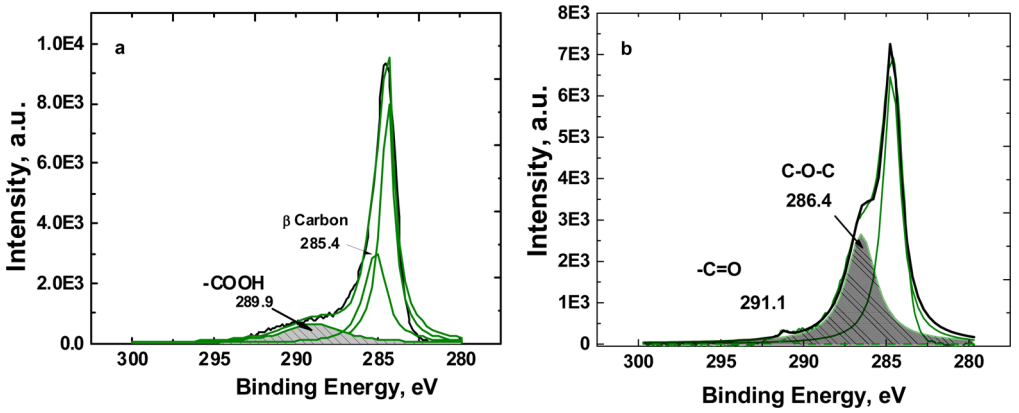

Figure 5. Peak deconvolution of high resolution C 1s spectra for (a) acid treated CNT (OCNT) and (b) aliphatic ether-OCNT.

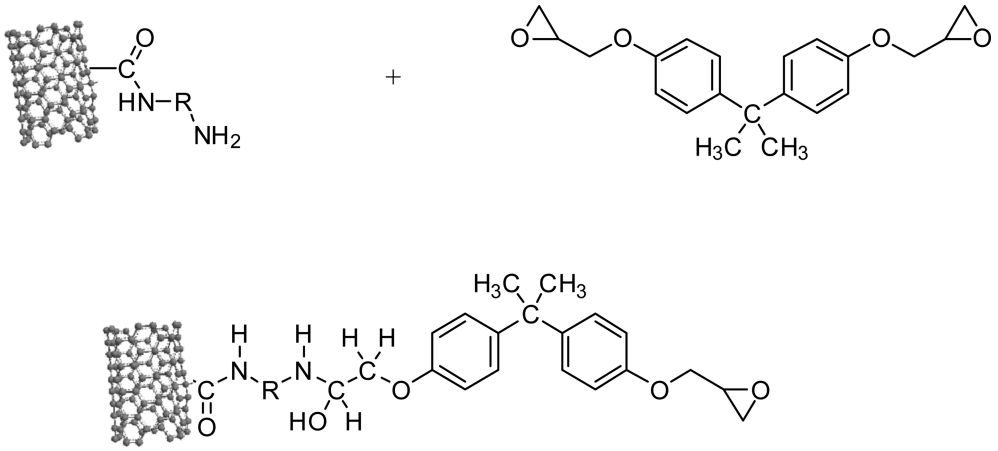

Figure 6. Reaction of amine functionalized CNT with diglycidyl ether of bisphenol A (DGEBA).

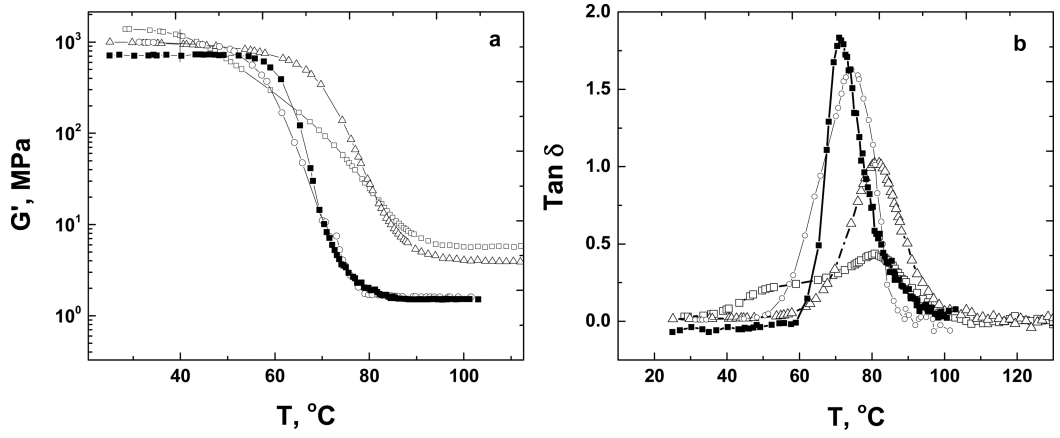

Figure 7. Storage shear moduli (a) and damping tan δ (b) of epoxy (■), 0.1 wt % C12-OCNT CNT/epoxy (Δ), aliphatic ether-OCNT (○), and aromatic-OCNT/epoxy (□) nanocomposites.

OCNT with binding energies of 284.6, 286.4, and 291.1 eV corresponding to graphitic carbon, ether linkage, and carbonyl/ester groups.[39−41] The area under the peak at higher binding energy corresponding to the carboxylic group of OCNT significantly decreased when OCNT reacted with aliphatic ether diamine. Figure 5b shows a peak at 286.4 eV corresponding to the ether linkage (C−O−C) with 39% peak area. The data suggests nearly complete reaction of aliphatic ether diamines with the carboxylic groups on the surface of OCNT. The area under higher binding energy peak shifted slightly to a higher binding energy of 291.1 eV, indicating the of presence of carbonyl/ester due to the carbonyl remaining after the reaction or carbonyl of acyl chloride.[42] The area under this peak significantly decreased to 0.5% of the total area.

CNT Epoxy Nanocomposites. *3.2.1. Dynamic and Thermal Properties.* Amine functionalized CNT were added to the epoxy resin to generate covalent bonding with the polymer matrix. The CNT epoxy nanocomposites are designed for maximum load transfer between low modulus epoxy resin matrix and high modulus CNT. Gonzalez-Domínguez et al.

dx.doi.org/10.1021/am5056849 | ACS Appl. Mater. Interfaces 2014, 6, 16621−16630

showed that the reactive amine group on the side wall of the CNT participates in the cross-linking reaction of the epoxy.[43] Jin et al. reported improved mechanical properties including dynamic modulus, fracture toughness, and 11 °C increase in glass transition temperature of dodecylamine treated CNT epoxy nanocomposites.[44] Putz et al. investigated the effects of the cross-linking density on the interfacial zone and its effects on a modified CNT epoxy resin nanocomposite.[45] The interfaces of the CNT were designed to explore the effects of interfacial dynamic and chain rigidity on the thermal and mechanical properties of the epoxy CNT nanocomposites. There is no report of a systematic study of the chemical structure of interfacial area on the bulk properties of CNT epoxy nanocomposites. Figure 6 shows the proposed the mechanism by which the chemical bonding between the diamine on the CNT surface and the epoxy matrix occurs.

Simulations of the surface modified CNT epoxy resin matrix demonstrated a 10-fold increase in the matrix shear modulus of the interface in the examined length scale.[46] Storage shear modulus, G', of epoxy and epoxy nanocomposites containing 1,12-diaminododecane, 4,7,10-trioxa-1,13-tridecanediamine, and 4,4′-(4,4′-methylenebis(4,1-phenylene)bis(methylene))-dianiline modified CNT were studied. Figure 7a,b shows the storage shear moduli and damping tan δ of the neat epoxy, 0.1 wt %, C12-OCNT/epoxy, aliphatic ether-OCNT epoxy, and aromatic Ph4-OCNT/epoxy nanocomposites. This study examines the effects of the interfacial rigidity and polarity on the mechanical properties of the epoxy nanocomposites. The storage shear moduli of all amine functionalized CNT epoxy nanocomposites were at least 1.3 times higher than that of the neat epoxy resin (Figure 7a). The aromatic modified CNT epoxy nanocomposites had the highest moduli below and above glass transition temperatures. The G' of the Ph4-OCNT epoxy nanocomposite was 1393 MPa, 1.9 times higher than that of the neat epoxy resin, 731 MPa, at 30 °C. The G' was very low in the rubbery state above T_g. The G' of the Ph4-OCNT epoxy resin was 5.9 MPa, which was a 3.98-fold increase at 100 °C compared to that of the neat epoxy resin matrix (1.5 MPa). This significant increase in shear moduli is attributed to the chain restriction due to the covalent bonding between the epoxy resin matrix and high modulus CNT through a rigid aromatic interface. The C12-OCNT epoxy nanocomposite also showed higher moduli below and above glass transition temperature. The C12-OCNT epoxy nanocomposite has a modulus of 989 MPa, which is a 1.35 times increase at 30 °C. The dynamic shear modulus of this nanocomposite was significantly higher at temperatures above T_g. The G' of the C12-OCNT epoxy nanocomposite showed a 2.48 times increase compared to that of the neat epoxy resin at 100 °C. Aliphatic ether-OCNT epoxy nanocomposite exhibited a higher modulus (993 MPa) below the glass transition temperature, in the same range as the C12-OCNT epoxy nanocomposites. Their G' was slightly higher or nearly the same as that of the epoxy resin nanocomposites above T_g, i.e., at 100 °C. The aliphatic ether amine modified CNT generated the most flexible interface with the epoxy resin matrix. It also demonstrated the least contribution to the modulus enhancement, especially above T_g.

The glass transition temperatures of all amine functionalized CNT epoxy nanocomposites were higher than the that of the neat epoxy resin by at least 3 °C (Figure 7b). The area under the tan δ damping peak decreased with incorporation of amine functionalized CNT to the epoxy resin matrix at an applied range of strain and frequency of 1 Hz. Tan δ is the ratio of loss modulus to storage modulus, G''/G'. A higher area under the tan δ peak suggests higher energy dissipation in the polymer system. Addition of stiffer CNT to the epoxy resin matrix resulted in a decrease in the area under the damping peak. In addition, this study demonstrates that the interface plays a role in the area under the damping peak. The CNT epoxy nanocomposite with the aliphatic ether interfacial structure shows high damping characteristics, possibly due to the flexible ether linkage, whereas the aromatic interface shows the lowest damping area, most likely due to the rigid aromatic structure. The area under the damping peak for the C12-OCNT epoxy nanocomposite was in between that of the flexible ether and rigid aromatic interface CNT epoxy nanocomposite.

Many studies reported an increase in damping characteristics of epoxy CNT nanocomposites caused by a stick−slip mechanism due to elastic mismatch and shear lag when the stress is above the critical value, resulting in polymer chain slippage from the CNT.[47−49] The main factors affecting the damping characteristic of CNT epoxy nanocomposites are reported as the critical shear stress, nanotube content, and CNT structural characterisitics.[35] Our prepared amine functionalized CNT epoxy nanocomposites do not show any increase in damping, rather a decrease in damping. These results suggest that the proposed slip−stick mechanism based on chain slippage on the CNT surface causing increased damping is absent. This could be attributed to the low concentration of CNTs (0.1 wt %), covalent bonding between the amine functionalized CNT and epoxy resin matrix, low applied frequency, or stress and strain below the critical value required for polymer chain slippage to occur.

The glass transition temperature of the neat epoxy was 71.2 °C, whereas aliphatic ether-OCNT, C12-OCNT, and aromatic functionalized CNT epoxy nanocomposites have T_g values of 74.4, 81.1, and 81.6 °C, respectively. The increase in the T_g is attributed to the contribution of functionalized CNT to the chain segmental motion. When CNT are covalently bonded to the epoxy resin matrix, the three-dimensional network requires higher thermal energy for onset of chain segmental motion compared to the neat polymer system. The aromatic modified CNT nanocomposites have the highest T_g, lowest area under the damping peak, and highest modulus. These property enhancements are attributed to the role of rigid interface covalently bonded to the three-dimensional network of epoxy resin. The aliphatic ether modified CNT exhibited the lowest T_g of the nanocomposites, a higher area under the damping peak, and a comparable improvement in G' compared to the 1,12-diaminododecane and aromatic modified CNT epoxy nanocomposites. This is possibly attributed to the highly flexible interface between CNT and the epoxy resin matrix.

1,12-Diaminododecane surface modified CNT with acid treated CNT (OCNT) and photo-oxidized CNT (POCNT) were prepared and incorporate into the epoxy resin to generate C12-OCNT and C12-POCNT epoxy nanocomposites. Figure 8 shows the storage shear modulus, and the tan δ data of C12-OCNT and C12-POCNT epoxy nanocomposites. The C12-OCNT epoxy nanocomposite shows a slightly higher modulus below T_g, but a more pronounced increase in the temperature range above the glass transition temperature. The T_g of the C12-OCNT nanocomposite was higher than the T_g of the C12-POCNT nanocomposite. The C12-OCNT epoxy nanocomposite had a modulus of 989 MPa vs 890 MPa for the C12-POCNT epoxy nanocomposite below T_g. The difference

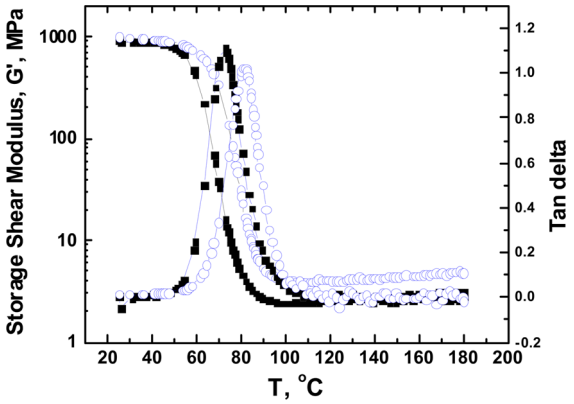

Figure 8. Storage shear moduli and damping tan δ of the C12-OCNT (■) and C12-POCNT (O) epoxy nanocomposites.

in modulus above T_g was more significant, 3.89 MPa vs 2.74 MPa for the C12-OCNT and C12-POCNT epoxy nanocomposites, respectively. XPS data showed significantly lower oxygen content on the POCNT surface and lower atomic nitrogen percentage on the amine modified POCNT. The lower modulus, lower T_g, and slightly higher area under the damping peak can be attributed to the lower density of functionalization due to lower available functional groups. This resulted in higher covalent bonding between the CNT and the epoxy resin matrix. This effect is more prominent at temperatures above T_g, where the polymer matrix has energy to undergo chain segmental motion, but the CNT thermal properties are not affected at this temperature range. The higher density of covalent bonding between the CNT and epoxy resin matrix results in hindering these motions and consequently larger effects in modulus at the temperatures above the glass transition temperature. The T_g of the C12-OCNT epoxy nanocomposite is 81.1 °C, whereas the T_g of the C12-POCNT epoxy nanocomposite was 72 °C. The increase in T_g is also attributed to the higher density of functionalization between the epoxy and CNT.

Table 2 summarizes the storage shear moduli ($<T_g$) of the carbon nanotube epoxy nanocomposites oxidized with acid (OCNT) and oxidized via photo-oxidation (POCNT) and then treated with the three types of diamines. The moduli of the epoxy CNT nanocomposites prepared from CNT with initial lower oxygen content were lower below and above the glass transition temperature. The moduli values for epoxy CNT nanocomposites containing a higher initial oxygen content and initial nitrogen content were higher both below and above the glass transition temperature for all epoxy CNT nanocomposites. The initial higher levels of oxygen content indicated initial higher oxygenated functional groups on the CNT surface. XPS also showed that amine functionalized CNT from acid treated CNT contained more nitrogen. Higher nitrogen content is an indication of higher density of amine end groups on the CNT interface, leading to more functional groups accessible for covalent bonding with the epoxy resin matrix.

Table 2. Storage Shear Moduli of Diamine Treated CNT Epoxy Nanocomposites with 1,12-Diaminododecane, 7,10-Trioxa-1,13-tridecanediamine, and 4,4′-(4,4′-Methylenebis(4,1-phenylene)bis(methylene))dianiline Treated CNT, Comparison of CNT Initially Acid Treated (OCNT) and Photo-oxidized (POCNT)

type of CNT functionalization in epoxy nanocomposite	storage shear modulus $<T_g$, MPa
neat epoxy	731 ± 75
Ph4-OCNT	1393 ± 207
Ph4-POCNT	1350 ± 170
aliphatic ether-OCNT	993 ± 104
aliphatic ether-POCNT	877 ± 150
C12-OCNT	989 ± 104
C12-POCNT	890 ± 76

Higher density of functionalization of OCNT leads to a higher stiffness and higher modulus of the epoxy CNT nanocomposites, however, the acid treatment could also result in decrease of aspect ratio. The lower aspect ratio results in improved dispersion which contributes to enhanced modulus. The POCNT has only been treated with UV light with minimal damage to CNT and effect on the aspect ratio. Therefore, higher aspect ratio CNT with more aggregation could result in epoxy CNT nanocomposites with lower modulus and mechanical properties.

3.2.2. SEM. The dispersions of all amine functionalized CNT in the epoxy resin matrix were evaluated by examination of the fractured surfaces with high resolution SEM. SEM has been widely used to evaluate the dispersion of CNT in the epoxy resin matrix.[29,30,32,34] Figure 9a,b,c shows the fractured surface of C12-OCNT, aliphatic ether-OCNT, and aromatic Ph4-OCNT epoxy nanocomposites. All CNT epoxy nanocomposite samples exhibited some degree of aggregation and nesting. However, the aromatic Ph4-OCNT epoxy nanocomposite showed significant improvements in the CNT dispersion, smaller CNT aggregate sizes, and less frequent aggregates compared to the C12-OCNT and aliphatic ether-OCNT epoxy nanocomposites (Figure 9c). The fractured surface of C12-OCNT epoxy nanocomposites showed some aggregation of CNT, whereas aggregate sizes were larger when aliphatic ether-OCNT was incorporated into the epoxy resin matrix (Figure 9a,b). This is in agreement with the improved properties of aromatic Ph4-OCNT epoxy nanocomposites compared to the C12-OCNT and aliphatic ether-OCNT epoxy nanocomposites.

All amine functionalized CNT exhibited good adhesion to the epoxy resin matrix on the examined fractured surfaces for all amine functionalized OCNT epoxy resin nanocomposites. Figure 10a,b shows fracture surfaces of aromatic Ph4-OCNT epoxy nanocomposite. Higher magnification (100 K) of the inside a small aggregate shows excellent adhesion of epoxy resin to the CNT. The epoxy resin covered outside of the aromatic Ph4-OCNT epoxy nanocomposite in areas 2 and 3 of Figure 10b. CNT bonded with epoxy resin was not completely pulled out and remained partially within the epoxy resin, Figure 10b area 1. This suggests improved load and stress transfer from the weak epoxy resin matrix to the high stiffness CNT and improved bonding between two components.

4. CONCLUSIONS

Surface functionalization of oxidized CNT with 1,12-diaminododecane, 4,7,10-trioxa-1,13-tridecanediamine and 4,4′-(4,4′-methylenebis(4,1-phenylene)bis(methylene))-dianiline were performed and verified by XPS and TGA. Acid treated CNT and photo-oxidized CNT were both modified with the series of diamines. Amine functionalized epoxy/CNT nanocomposites were prepared and exhibited improved dynamic shear moduli and glass transition temperatures

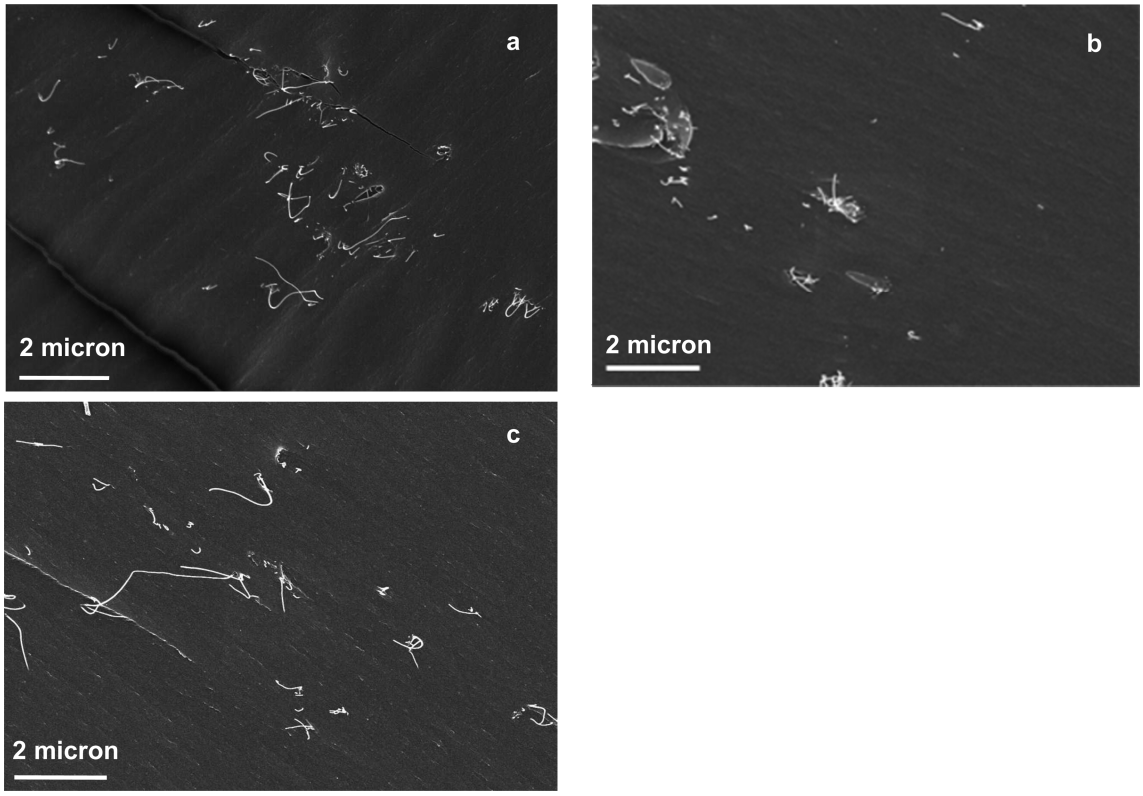

Figure 9. HR-SEM micrographs of the fractured surface of C12-OCNT (a), aliphatic-OCNT (b), and (c) aromatic Ph4-OCNT epoxy nanocomposites.

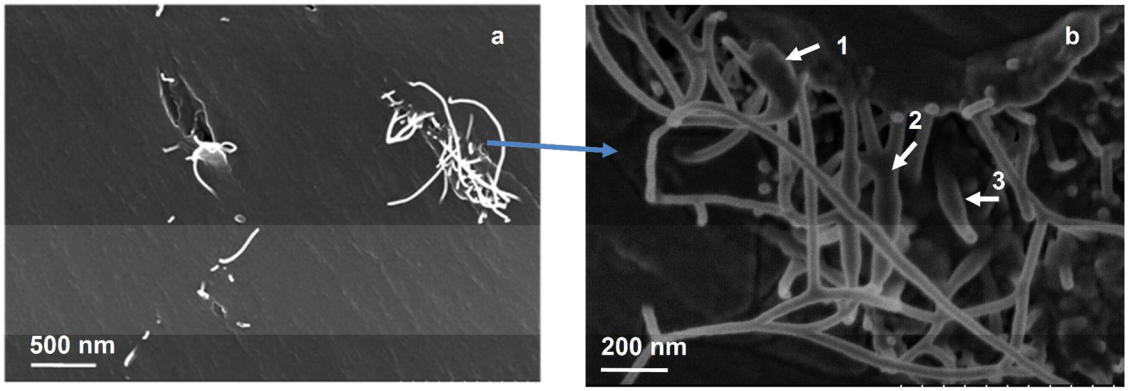

Figure 10. HR-SEM micrograph of aromatic Ph4-OCNT epoxy nanocomposite (a) and higher magnification of the epoxy covered CNT (b).

compared to neat epoxy resin. The highest improvement was found when aromatic interface between CNT and epoxy resin matrix was used. The dynamic shear modulus showed greater improvement at temperatures above the glass transition temperature for all nanocomposites. The storage shear moduli of the amine functionalized epoxy/CNT nanocomposite with acid treated CNT were higher than the photo-oxidized ones. This is attributed to the lower density of functionalization due to the lower initial oxygenated functional sites on the photo-oxidized CNT. Improvements in the dispersion of aromatic diamine modified CNT compared to the aliphatic alkyl and ether diamines was observed using SEM.

AUTHOR INFORMATION

Corresponding Author

*M. Yoonessi. E-mail: mitra.yoonessi@gmail.com.

Notes

The authors declare no competing financial interest.

ACKNOWLEDGMENTS

The NASA Aeronautics-Subsonic Fixed Wing Program (Contract NNC07BA13B) provided financial support for this work. NASA summer faculty fellowship program and Dr. Kankam are thanked. Ms. Dorothy Lokco and Dave Hull are thanked for their support for XPS, HR-TEM, and FE-SEM.

REFERENCES

(1) Winey, K. I.; Vaia, R. A. Polymer Nanocomposites. *MRS Bull.* **2007**, *32*, 314−322.

(2) Gintret, M. J.; Jana, S. C.; Miller, S. G. A Novel Strategy for Nanoclay Exfoliation in Thermoset Polyimide Nanocomposite Systems. *Polymer* **2007**, *48*, 4166−4173.

(3) Yoonessi, M.; Toghiani, H.; Daulton, T. L.; Lin, J.-S.; Pittman, C. U., Jr. Clay Delamination in Clay/Poly(dicyclopentadiene) Nanocomposites Quantified by Small Angle Neutron Scattering and High-Resolution Transmission Electron Microscopy. *Macromolecules* **2005**, *38*, 818−831.
(4) Drummy, L. F.; Koerner, H.; Farmer, K.; Tan, A.; Farmer, B. L.; Vaia, R. A. High-Resolution Electron Microscopy of Montmorillonite and Montmorillonite/Epoxy Nanocomposites. *J. Phys. Chem. B* **2005**, *109*, 17868−17878.
(5) Rajoria, H.; Jalili, N. Passive Vibration Damping Enhancement Using Carbon Nanotube-Epoxy Reinforced Composites. *Compos. Sci. Technol.* **2005**, *65*, 2079−2093.
(6) Gelves, G. A.; Al-Saleh, M. H.; Sundararaj, U. Highly Electrically Conductive and High Performance EMI Shielding Nanowire/Polymer Nanocomposites by Miscible Mixing and Precipitation. *J. Mater. Chem.* **2011**, *21*, 829−836.
(7) Liang, J.; Wang, Y.; Huang, Y.; Ma, Y.; Liu, Z.; Cai, J.; Zhang, C.; Gao, H.; Chen, Y. Electromagnetic Interference Shielding of Graphene/Epoxy Composites. *Carbon* **2009**, *47*, 922−925.
(8) Ajayan, P. M.; Stephan, O.; Colliex, C.; Trauth, D. Aligned Carbon Nanotube Arrays Formed by Cutting a Polymer Resin−Nanotube Composite. *Science* **1994**, *265*, 1212−1214.
(9) Suhr, J.; Koratkar, N.; Keblinski, P.; Ajayan, P. Viscoelasticity in Carbon Nanotube Composites. *Nat. Mater.* **2005**, *4*, 134−137.
(10) Bekyarova, E.; Thostenson, E. T.; Yu, A.; Kim, H.; Gao, J.; Tang, J.; Hahn, H. T.; Chou, T.-W.; Itkis, M. E.; Haddon, R. C. Multiscale Carbon Nanotube-Carbon Fiber Reinforcement for Advanced Epoxy Composites. *Langmuir* **2007**, *23*, 3970−3974.
(11) Vennerberg, D.; Rueger, Z.; Kessler, M. R. Effect of Silane Structure on the Properties of Silanized Multiwalled Carbon Nanotube-Epoxy Nanocomposites. *Polymer* **2014**, *55*, 1854−1865.
(12) Singh, B. P.; Saini, K.; Choudhary, V.; Teotia, S.; Pande, S.; Saini, P.; Mathur, R. B. Effect of Length of Carbon Nanotubes on Electromagnetic Interference Shielding and Mechanical Properties of Their Reinforced Epoxy Composites. *J. Nanopart. Res.* **2014**, *16*, 1−11.
(13) Gogosti, Y. *Carbon Nanomaterials*; Taylor & Francis: New York, NY, 2006.
(14) Baughman, R. H.; Zakhidov, A. A.; de Heer, W. A. Carbon Nanotubes—The Route toward Applications. *Science* **2002**, *2*, 787−792.
(15) Chen, J.; Hamon, M. A.; Hu, H.; Chen, Y.; Rao, A. M.; Eklund, P. C.; Haddon, R. C. Solution Properties of Single-Walled Carbon Nanotubes. *Science* **1998**, *282*, 95−98.
(16) Ebbesen, T. W.; Ajayan, P. M. Large-Scale Synthesis of Carbon Nanotubes. *Nature* **1992**, *358*, 220−222.
(17) Bajpai, V.; Dai, L.; Ohashi, T. Large-Scale Synthesis of Perpendicularly Aligned Helical Carbon Nanotubes. *J. Am. Chem. Soc.* **2004**, *126*, 5070−5071.
(18) Ma, J.; Larsen, R. M. Comparative Study on Dispersion and Interfacial Properties of Single Walled Carbon Nanotube/Polymer Composites Using Hansen Solubility Parameters. *ACS Appl. Mater. Interfaces* **2013**, *5*, 1287−1293.
(19) Tseng, C.-H.; Wang, C.-C.; Chen, C.-Y. Functionalizing Carbon Nanotubes by Plasma Modification for the Preparation of Covalent-Integrated Epoxy Composites. *Chem. Mater.* **2007**, *19*, 308−315.
(20) Nanda, J.; Maranville, C.; Bollin, S. C.; Sawall, D.; Ohtani, H.; Remillard, J. T.; Ginder, J. M. Thermal Conductivity of Single-Wall Carbon Nanotube Dispersions: Role of Interfacial Effects. *J. Phys. Chem. C* **2008**, *112*, 654−658.
(21) Miller, S. G.; Williams, T. S.; Baker, J. S.; Solá, F.; Lebron-Colon, M.; McCorkle, L. S.; Wilmoth, N. G.; Gaier, J.; Chen, M.; Meador, M. A. Increased Tensile Strength of Carbon Nanotube Yarns and Sheets through Chemical Modification and Electron Beam Irradiation. *ACS Appl. Mater. Interfaces* **2014**, *6*, 6120−6126.
(22) Liu, J.; Rinzler, A.; Dai, H.; Hafner, J. H.; R. Bradley, K.; Boul, P. J.; Lu, A.; Iverson, T.; Shelimov, K.; Huffman, C. B.; Rodriguez-Macias, F.; Shon, Y.-S.; Lee, T. R.; Colbert, D. T.; Smalley, R. E. Fullerene Pipes. *Science* **1998**, *280*, 1253−1256.
(23) Datsyuk, V.; Kalyva, M.; Papagelis, K.; Parthenios, J.; Tasis, D.; Siokou, A.; Kallitsis, I.; Galiotis, C. Chemical oxidation of Multiwalled Carbon Nanotubes. *Carbon* **2008**, *46*, 833−840.
(24) Lebrón-Colón, M.; Meador, M. A.; Lukco, D.; Solá, F.; Santos-Pérez, J.; McCorkle, L. S. Surface Oxidation Study of Single Wall Carbon Nanotubes. *Nanotechnology* **2011**, *11*, 455707.
(25) Lebrón-Colón, M.; Meador, M. A.; Gaier, J. R.; Solá, F.; Scheiman, D. A.; McCorkle, L. S. Reinforced Thermoplastic Polyimide with Dispersed Functionalized Single Wall Carbon Nanotubes. *ACS Appl. Mater. Interfaces* **2010**, *2*, 669−76.
(26) Vaisman, L.; Marom, G.; Wagner, H. D. Dispersions of Surface-Modified Carbon Nanotubes in Water-Soluble and Water-Insoluble Polymers. *Adv. Funct. Mater.* **2006**, *16*, 357−363.
(27) Yi, W.; Malkovskiy, A.; Xu, Y.; Wang, X.-Q.; Sokolov, A. P.; Lebron Colon, M.; Meador, M.; Pang, Y. Polymer Conformation-Assisted Wrapping of Single-Walled Carbon Nanotube: The Impact of cis-Vinylene Linkage. *Polymer* **2010**, *51*, 475−481.
(28) Spitalsky, Z.; Tasis, D.; Papagelis, K.; Galiotis, C. Carbon Nanotube−Polymer Composites: Chemistry, Processing, Mechanical and Electrical Properties. *Prog. Polym. Sci.* **2010**, *35*, 357−401.
(29) Zhu, J.; Kim, J.; Peng, H.; Margrave, J. L.; Khabashesku, V. N.; Barrera, E. V. Improving the Dispersion and Integration of Single-Walled Carbon Nanotubes in Epoxy Composites through Functionalization. *Nano Lett.* **2003**, *3*, 1107−1113.
(30) Kim, J. T.; Kim, H.-C.; Kim, S.-K.; Kathi, J.; Rhee, K.-Y. 3-Aminopropyltriethoxysilane Effect on Thermal and Mechanical Properties of Multi-Walled Carbon Nanotubes Reinforced Epoxy Composites. *J. Compos. Mater.* **2009**, *43*, 2533−2541.
(31) Lavorgna, M.; Romeo, V.; Martone, A.; Zarrelli, M.; Giordano, M.; Buonocore, G. G.; Qu, M. Z.; Fei, G. X.; Xia, H. S. Silanization and Silica Enrichment of Multiwalled Carbon Nanotubes: Synergistic Effects on the Thermal-Mechanical Properties of Epoxy Nanocomposites. *Eur. Polym. J.* **2013**, *49*, 428−438.
(32) Vennerberg, D.; Hall, R.; Kessler, M. R. Supercritical Carbon Dioxide-Assisted Silanization of Multi-Walled Carbon Nanotubes and Their Effect on the Thermo-Mechanical Properties of Epoxy Nanocomposites. *Polymer* **2014**, *55*, 4156−4163.
(33) Bekyarova, E.; Thostenson, E. T.; Yu, A.; Itkis, M. E.; Fakhrutdinov, D.; Chou, T.-W.; Haddon, R. C. Functionalized Single-Walled Carbon Nanotubes for Carbon Fiber-Epoxy Composites. *J. Phys. Chem. C* **2007**, *111*, 17865−17871.
(34) Gulotty, R.; Castellino, M.; Jagdale, P.; Tagliaferro, A.; Balandin, A. A. Effects of Functionalization on Thermal Properties of Single-Wall and Multi-Wall Carbon NanotubePolymer Nanocomposites. *ACS Nano* **2013**, *7*, 5114−5121.
(35) Ramanathan, T.; Fisher, F. T.; Ruoff, R. S.; Brinson, L. C. Amino-Functionalized Carbon Nanotubes for Binding to Polymers and Biological Systems. *Chem. Mater.* **2005**, *17*, 1290−1295.
(36) Prolongo, S. G.; Gude, M. R.; Ureña, A. Improving the Flexural and Thermomechanical Properties of Amino-Functionalized Carbon Nanotube/Epoxy Composites by Using a Pre-Curing Treatment. *Compos. Sci. Technol.* **2011**, *71*, 765−771.
(37) Tseng, C.-H.; Wang, C.-C.; Chen, C.-Y. Functionalizing Carbon Nanotubes by Plasma Modification for the Preparation of Covalent-Integrated Epoxy Composites. *Chem. Mater.* **2007**, *19*, 308−315.
(38) Gonzalez-Domínguez, J. M.; Gonzalez, M.; Anson-Casaos, A.; Díez-Pascual, A. M.; Gomez, M. A.; Martínez, M. T. Effect of Various Aminated Single-Walled Carbon Nanotubes on the Epoxy Cross-Linking Reactions. *J. Phys. Chem. C* **2011**, *115*, 7238−7248.
(39) Lakshminarayanan, P. V.; Toghiani, H.; Pittman, C. U., Jr. Nitric Acid Oxidation of Vapor Grown Carbon Nanofibers. *Carbon* **2004**, *42*, 2433−2442.
(40) Viswanathan, H.; Wang, Y.-Q.; Audi, A.; Allen, P. J.; Sherwood, P. M. A. X-ray Photoelectron Spectroscopic Studies of Carbon Fiber Surfaces. 24. Interfacial Interactions between Polyimide Resin and Electrochemically Oxidized PAN-based Carbon Fibers. *Chem. Mater.* **2001**, *13*, 1647−1655.

(41) Zielke, U.; Huttinger, K. J.; Hoffman, W. P. Surface-Oxidized Carbon Fibers: IV. Interaction with High-Temperature Thermoplastics. *Carbon* **1996**, *34*, 1015−26.
(42) Kassis, C. M.; Steehler, J. K.; Linton, R. W. Characterization of 1,1-Dihydroperfluorooctyl Acrylate (PFOA) by XPS. *Surf. Sci. Spectra* **1994**, *3*, 299−306.
(43) Gonzalez-Domínguez, J. M.; Gonzalez, M.; Anson-Casaos, A.; Díez-Pascual, A. M.; Gomez, M. A.; Martínez, M. T. Effect of Various Aminated Single-Walled Carbon Nanotubes on the Epoxy Cross-Linking Reactions. *J. Phys. Chem. C* **2011**, *115*, 7238−7248.
(44) Jin, F.-L.; Ma, C.-J.; Park, S.-J. Thermal and Mechanical Interfacial Properties of Epoxy Composites Based on Functionalized Carbon Nanotubes. *Mater. Sci. Eng., A* **2011**, *528*, 8517−8522.
(45) Putz, K. W.; Palmeri, M. J.; Cohn, R. B.; Andrews, R.; Brinson, L. C. Effect of Cross-Link Density on Interphase Creation in Polymer Nanocomposites. *Macromolecules* **2008**, *41*, 6752−6756.
(46) Coto, B.; Antia, I.; Barriga, J.; Blanco, M.; Sarasua, J.-R. Influence of the Geometrical Properties of the Carbon Nanotubes on the Interfacial Behavior of Epoxy/CNT Composites: A Molecular Modeling Approach. *Comput. Mater. Sci.* **2013**, *79*, 99−104.
(47) Alva, A.; Raja, S. Damping Characteristics of Epoxy-Reinforced Composite with Multiwall Carbon Nanotubes. *Mech. Adv. Mater. Struct.* **2014**, *21*, 197−206.
(48) Ullah Khan, S.; Li, C. Y.; Siddiqui, N. A.; Kim, J.-K. Vibration Damping Characteristics of Carbon Fiber-Reinforced Composites Containing Multi-Walled Carbon Nanotubes. *Compos. Sci. Technol.* **2011**, *71*, 1486−1494.
(49) Zhou, X.; Shin, E.; Wang, K. W.; Bakis, C. E. Interfacial Damping Characteristics of Carbon Nanotube-based Composites. *Compos. Sci. Technol.* **2004**, *64*, 2425−2437.